Environmental Microbiology (2009) **11**(10), 2710–2719 doi:10.1111/j.1462-2920.2009.01998.x

Microbial diversity in modern marine stromatolites, Highborne Cay, Bahamas

Laura K. Baumgartner,[1†] John R. Spear,[2] Daniel H. Buckley,[3] Norman R. Pace,[4] R. Pamela Reid,[5] Christophe Dupraz[1] and Pieter T. Visscher[1*]

[1]*Department of Marine Sciences, University of Connecticut, Groton, CT 06340, USA.*
[2]*Division of Environmental Science and Engineering, Colorado School of Mines, Golden, CO 80401, USA.*
[3]*Department of Crop and Soil Sciences, Cornell University, Ithaca, NY 14853, USA.*
[4]*Department of Molecular, Cellular and Developmental Biology, University of Colorado, Boulder, Boulder, CO 80309, USA.*
[5]*Marine Geology and Geophysics, Rosenstiel School of Marine and Atmospheric Science, University of Miami, Miami, FL 33149, USA.*

Summary

Living marine stromatolites at Highborne Cay, Bahamas, are formed by microbial mat communities that facilitate precipitation of calcium carbonate and bind and trap small carbonate sand grains. This process results in a laminated structure similar to the layering observed in ancient stromatolites. In the modern marine system at Highborne Cay, lamination, lithification and stromatolite formation are associated with cycling between three types of microbial communities at the stromatolite surface (Types 1, 2 and 3, which range from a leathery microbial mat to microbially fused sediment). Examination of 923 universal small-subunit rRNA gene sequences from these communities reveals that taxonomic richness increases during transition from Type 1 to Type 3 communities, supporting a previous model that proposed that the three communities represent different stages of mat development. The phylogenetic composition also changes significantly between these community types and these community changes occur in concert with variation in biogeochemical rates. The dominant bacterial groups detected in the stromatolites include *Alphaproteobacteria*, *Planctomycetes*, *Cyanobacteria* and *Bacteroidetes*. In addition, the stromatolite communities were found to contain novel cyanobacteria that may be uniquely associated with modern marine stromatolites. The implications of these findings are discussed in the context of current models for stromatolite formation.

Received 2 February, 2009; accepted 4 June, 2009. *For correspondence. E-mail pieter.visscher@uconn.edu; Tel. (+) 860 405 9159; Fax (+) 860 405 9153. †Present address: Department of Molecular, Cellular and Developmental Biology, University of Colorado, Boulder, Boulder, CO 80309, USA.

Introduction

Stromatolites are laminated sedimentary microbial ecosystems that were common throughout the Precambrian, and fossil stromatolites provide some of the earliest evidence of life. Modern stromatolites in Shark Bay, Australia (Macintyre *et al*., 2000; Burns *et al*., 2004; 2005; Goh *et al*., 2006) and Highborne Cay, Bahamas (e.g. Visscher *et al*., 1998; 2000; 2002; Macintyre *et al*., 2000; Reid *et al*., 2000; Decho *et al*., 2005; Dupraz and Visscher, 2005; Visscher and Stolz, 2005; Andres *et al*., 2006) represent a living link to these ancient ecosystems and have been studied to provide insights on the ecology and biogeochemistry of their Precambrian counterparts.

Lamination in Highborne Cay stromatolites is thought to result from a cycling of three distinct microbial surface communities, which have been previously described through biogeochemical and microscopic observations (e.g. Reid *et al*., 2000). Type 1 microbial mats are dominated by filamentous cyanobacteria (identified as *Schizothrix* spp. by light microscopy), which trap and bind carbonate grains (ooids). This community is characterized by rapid production of new extracellular polymeric substances (EPS) (Reid *et al*., 2000; Decho *et al*., 2005), which bind calcium and thereby inhibit calcium carbonate precipitation (Dupraz and Visscher, 2005; Braissant *et al*., 2007). Type 1 surface mats mature into Type 2 surface mats after a hiatus in sediment accretion of a few days or weeks (Reid *et al*., 2000). During the formation of Type 2 surface mats, mineral precipitation forms a thin microcrystalline calcium carbonate (micrite) crust at the mat surface (Visscher *et al*., 2000). Cyanobacteria are less conspicuous in Type 2 mats and these mats contain a diversity of heterotrophic organisms and copious amounts of EPS (Reid *et al*., 2000; Decho *et al*., 2005; Braissant *et al*., 2007). A resumption of sediment accretion may cause cyanobacteria from Type 2 microbial mats to

migrate upwards through newly deposited sediment (ooids). The cyanobacteria trap and bind this new sediment, and cause the surface of the stromatolite to revert to a Type 1 community. If, however, the hiatus in sediment accretion extends to periods of weeks to months, a Type 3 surface mat forms (Reid *et al*., 2000). Type 3 mats are characterized by an abundance of endolithic coccoid cyanobacteria identified as *Solentia* sp. by light microscopy (Macintyre *et al*., 2000). Microbial precipitation of micrite in *Solentia* boreholes crossing between adjacent grains fuses grains together, forming cemented layers (Macintyre *et al*., 2000). As in the Type 2 mats, a resumption of sediment accretion on the stromatolite surface will cause the formation of a new Type 1 community at the stromatolite surface. Subsurface lamination in Highborne Cay stromatolites records a cycling of these three surface communities with alternating formation of trapped and bound sediment, micritic crusts and fused grain layers. The sequence of these three different mineralogical features results in the layered structure of the stromatolite (Reid *et al*., 2000).

The three surface communities exhibit different degrees of lithification and microscopically conspicuous changes in community composition (Reid *et al*., 2000). Mechanisms have been identified through which changes in microbial community composition can affect the potential for lithification (the formation of solid rock from loose sediment) in microbial mats (Visscher *et al*., 2000; Dupraz and Visscher, 2005). However, detailed information on community composition for the Highborne Cay stromatolite system is currently lacking.

The objective of this study was to explore the formation of Highborne Cay stromatolites using molecular and biogeochemical techniques to examine microbial diversity in each of the three surface mat types. In addition, we sought a broader understanding of the composition of the mat communities to gain insight into the mechanism of stromatolite lithification and to address fundamental questions regarding microbial populations and processes involved in stromatolite formation.

Results

Physical description of mats by type

The stromatolite microbial mat samples used in this study (Fig. 1) were similar to those previously described for each type of surface community (e.g. Reid *et al*., 2000). The Type 1 surface community mats were leathery, caramel-coloured, with bound sand grains and EPS

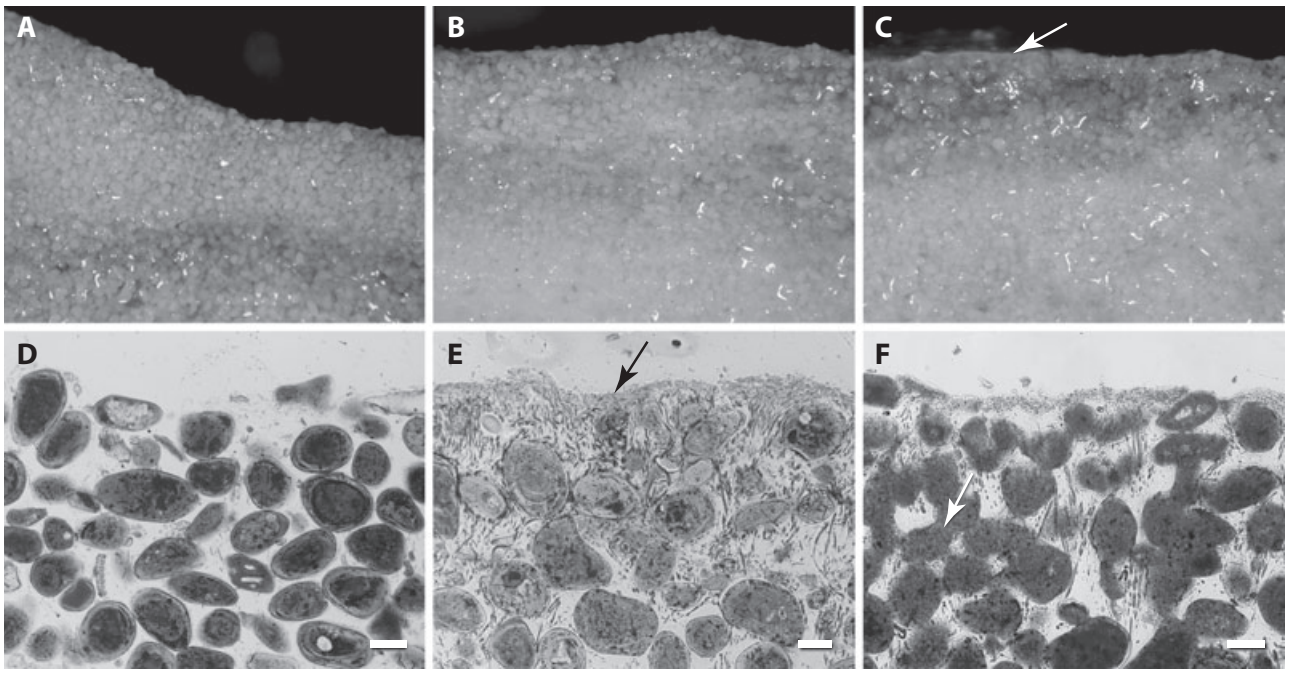

Fig. 1. Cross-sections of the three different surface mat types used in this study as viewed with stereo microscopy (A, C and E) and light microscopy of embedded thin sections stained with methylene blue (stains cyanobacteria) (B, D and F) of stromatolite heads used in this study (shown in cross-section). The caramel-coloured section at the very surface was sampled in all cases.
A and B. Type 1 surface mat.
C and D. Type 2 surface mats with micritized calcium carbonate precipitation at the surface (indicated by the arrow in D).
E and F. Type 3 surface mat with fused sediment grains below the surface (indicated by the arrow in E).
Bars: 100 μm scale bars.

Table 1. Biogeochemical characteristics of mat layers.

Sample	O_2* penetration (mm)	O_2* (% saturation)	S^{2-}* (μM)	pH*	PS (μM min^{-1} m^{-2})	AR (μM min^{-1} m^{-2})	SR (μM h^{-1} m^{-2})
Mat Type 1	10 ± 1.4^a	335 ± 55^a	35 ± 10^a	8.9 ± 0.2^a	167 ± 33^a	92 ± 25	65 ± 13^a
Mat Type 2	4.5 ± 0.8^b	554 ± 68^b	193 ± 23^b	9.4 ± 0.3^b	265 ± 37^b	130 ± 37	736 ± 128^b
Mat Type 3	4.7 ± 0.9^b	519 ± 84^b	135 ± 44^b	9.2 ± 0.3^b	241 ± 38^b	100 ± 27	565 ± 101^b

*These values are expressed as the maximum value observed in each mat profile.
Values are means ($n = 6$–8) with standard deviations. Superscripts are used to indicate means that differ significantly within each column, with means that are significantly different from each other indicated by different superscripts (*t*-test, $P < 0.005$). PS indicates photosynthetic rate in terms of O_2 production, AR indicates aerobic respiration rate in terms of O_2 consumption, and SR indicates sulfate reduction rate in terms of S^{2-} production. O_2 profiles were measured until the concentration was zero for at least five observations (i.e. 5–12 mm depth); S^{2-} profiles were measured in the upper 15 mm, until there was no or only a little increase of the concentration with depth (see Visscher *et al*., 1998; 2002). PS and AR were measured until the rates equalled zero (which coincides with the depth of O_2 penetration). SR were measured in the upper 25–30 mm, which reflects > 90% of the total sulfate reduction rate (see Visscher *et al*., 2000; 2002).

(Fig. 1A and D). The caramel-coloured surfaces of the Type 1 mats were sampled for this study, which corresponded to the uppermost 0.8–1.6 mm of the stromatolite. The Type 2 surface community mats were less pliable, with a caramel-coloured surface layer (1 mm thick) topped with a thin carbonate crust (20–60 μm thick) (Fig. 1B and E). The caramel-coloured surfaces of the Type 2 mats were sampled for this study, which comprised the uppermost 0.8 mm of the stromatolite. The Type 3 surface community mats were more brittle, with a thin micritic curst (Fig. 1C and F) underlain by a layer of fused carbonate sand grains (visible in thin section). The caramel- and green-coloured surfaces of the Type 3 mats were sampled for this study, which corresponded to the uppermost 3 mm of the stromatolite.

Biogeochemistry

Microelectrode and other biogeochemical analysis provided insight into the chemical environment and microbial activities in each of the three mat types. The biogeochemical characteristics of Type 1 mats differed significantly in many respects from those in the Type 2 and Type 3 mats, while no significant differences were observed between the latter two mat types (Table 1). Type 2 and Type 3 mats had significantly higher concentrations of oxygen and sulfide, and rates of photosynthesis and sulfate reduction than Type 1 (Table 1). Type 1 mats also had lower pH than either Type 2 or Type 3 mats (Table 1), possibly reflecting the lower photosynthetic rates in Type 1 mats. Despite their higher O_2 concentrations, Type 2 and 3 mats have shallower O_2 penetration than Type 1 mats (Table 1). However, aerobic respiration rates were not significantly different between the mat types (Table 1), suggesting that differences in the maximum depth of O_2 penetration between mat layers largely result from reduction of O_2 by S^{2-}. This oxygen reduction by sulfide includes both consumption by sulfide-oxidizing bacteria and chemical sulfide oxidation. Furthermore, since chemical sulfide oxidation rates in seawater are very low (i.e. $\tau = 24$ h; Zhang, 2000), microbial sulfide oxidation possibly accounts for the bulk of the sulfide removal. The observation of sulfide removal by oxygen in Type 2 and 3 mats is supported by the 9- to 12-fold higher sulfate reduction rates in Type 2 and 3 mats compared with Type 1 mats (Table 1). The shallower depth of O_2 penetration further suggests a very tight coupling of oxygen-producing and -consuming processes (i.e. aerobic respiration and sulfide oxidation).

Analysis of mat community composition

DNAs from each surface mat type and a water sample were extracted and amplified with nominally universal small subunit (SSU) rDNA polymerase chain reaction (PCR) primers (see *Experimental procedures*). A total of 923 clones were sequenced from the three mat communities and the water sample. The libraries were optimized for analysis in DOTUR by removing the few eukaryotic sequences and shorter bacterial/archaeal sequences (Table 2). Most (77%) of the stromatolite sequences are < 95% identical to sequences in GenBank (approximately genus-level identity, Fig. 2). In contrast, only ~30% of the SSU rRNA sequences recovered from the water column are < 95% identical to known sequences (Fig. 2). These results indicate that the stromatolites contain a deeper reservoir of novel genetic diversity than that in the water column, although both environments are undersampled. The unique nature of the stromatolite sequences minimized our ability to make lower-level (genus, species) taxonomic identifications of many of the community constituents. Moreover, no sequences were shared between libraries from the mat samples and the water, indicating the distinct character of the mat communities from the water community.

Estimates of taxonomic richness showed that diversity increased in the progression from Type 1 to Type 3 mats (Fig. 3, Table 2), and the difference between Type 1 and Type 3 communities was significant when all sequences

Table 2. Diversity estimates for mat samples calculated from SSU rRNA gene libraries (OTU defined at a 0.03 dissimilarity cut-off).

Sample	Total sequences	Sequences in analysis	OTU	Ace	Chao1	Chao1 95% confidence interval
Mat Type 1	251	224	128	276	229	185/306
Mat Type 2	251	240	133	326	274	212/384
		224	127	265	265	204/376
Mat Type 3	350	328	181	484	398	313/538
		224	139	364	364	266/539
All Mat Types		792	368	804	750	634/915
		224	152	471	471	335/708
Water	71	68	31	58	69	43/157

Some sequences were removed for diversity analysis because they did not fit well in the chosen region of the alignment (e.g. they were eukaryotic, or did not fully cover the chosen region). Results for mat samples are provided at different levels of sampling effort (i.e. for all sequences and after 224 sequences) to facilitate direct comparison between samples.

are considered in the analysis (as indicated by the 95% confidence intervals for Chao1, Table 2). Sampling intensity can influence the value of the Chao1 estimator, however, and to control for this effect an equal number of sequences corresponding to the size of the smallest library were randomly sampled from each library. This analysis revealed that the richness of the Type 1 mats was lower (Table 2) than that of the entire stromatolite community (i.e. Type 1 + Type 2 + Type 3). This result was significant: richness increases during progression of mat development. In addition, the increase in richness between Type 1 and Type 2 mats occurred in parallel with significant increases in lithification (Fig. 1), the sulfate reduction rate and the photosynthetic rate (Table 1, Fig. 4).

Differences in community composition between the mat types were analysed with UniFrac and ∫-LibShuff. These statistical tests revealed differences between all mat types and between mat and water column communities, and these results were significant (∫-LibShuff, $P = 0.0000$, UniFrac phylogenetic and pairwise tests, $P = 0.00$). Operational taxonomic unit (OTU) clustering was performed with DOTUR and sortX, and both indicated that Type 2 and 3 mats are more similar to each other than either is to the Type 1 mats [OTUs shared between mat types (DOTUR, sortX): Type 2 to 3: 33, 46; Type 1 to 2: 5, 20; Type 1 to 3: 19, 34] (the most abundant OTUs from sortX are shown in Fig. 5). This result is supported by a jackknifed UPGMA tree (1000 replicates) generated with UniFrac (Fig. 6A). Additionally, the libraries from Highborne Cay stromatolites were compared with previously published libraries from modern stromatolites in Shark Bay, Australia (Burns *et al*., 2004; Papineau *et al*., 2005; Goh *et al*., 2006). The Highborne Cay libraries were distinct from those from Shark Bay (Fig. 6B).

Phylogenetic analysis

The sequences from each library were analysed to determine the phylogenetic associations of the OTUs detected, and these results are summarized in Table 3 and Fig. 5 (see *Experimental procedures*). The majority of

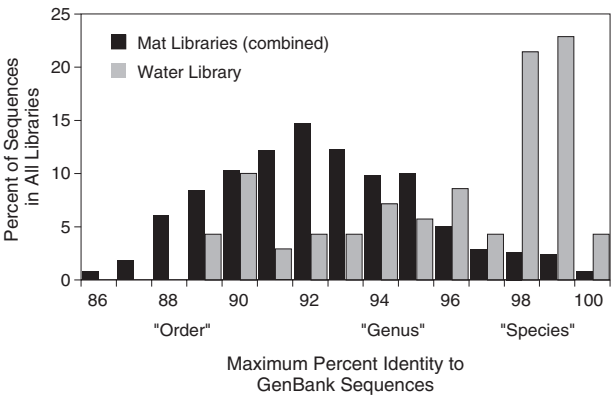

Fig. 2. Sequence identity for all of the sequences sampled in this study relative to sequences currently present in GenBank. Mat libraries are indicated by black bars and water column libraries are denoted by grey bars.

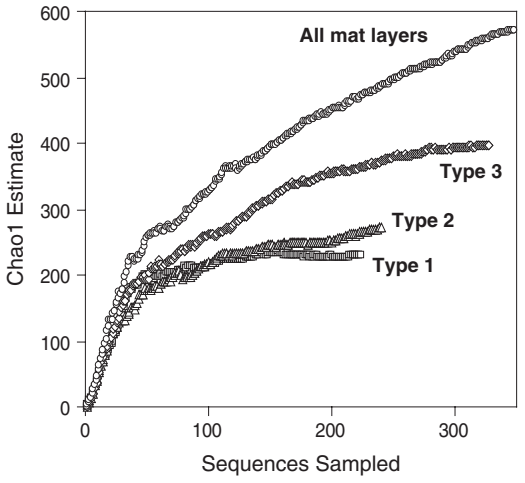

Fig. 3. Collection curves of estimated taxonomic richness (Chao1, 97% OTU) for SSU rRNA clone libraries from across all mat samples and from each mat type.

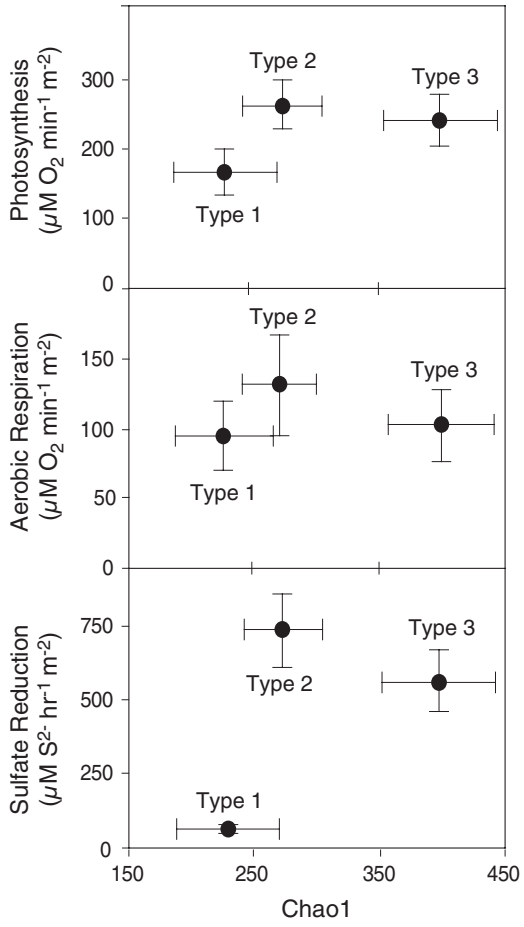

Fig. 4. Differences between mat types as a function of species richness and observed metabolic rates. Values are presented as means ($n = 5$ or 6 for metabolic rates) and standard deviation.

sequences from each library are bacterial, with archaeal sequences representing 0–1.4% and eukaryotic sequences (mostly from nematodes, with two dinoflagellate sequences and two sequences related to the alga *Acetabularia* sp.) representing 0–4.4% of the total sequences in each library (Table 3). Sequences from the *Alphaproteobacteria*, *Planctomycetes* and *Cyanobacteria* each comprised > 10% of all three libraries from the stromatolite mats. The alphaproteobacterial sequences in stromatolite samples were mostly from the *Rhodobacteraceae* and from several novel groups that did not belong to any currently recognized order within the *Alphaproteobacteria*. Several of the dominant alphaproteobacterial OTUs were only observed in mat Types 2 and 3 (Fig. 5). The majority of the *Planctomycetes* sequences grouped with members of the WPS-1 group. Finally, *Bacteroidetes*, mainly *Flexibacteraceae*, comprised 18% of the library from the Type 1 surface mats. Nearly 11% of these sequences belonged to a single OTU, a novel group within the *Flexibacteraceae* that dominates the Type 1 mat library (Fig. 5).

Cyanobacteria are microscopically conspicuous in the Highborne Cay stromatolite surface mats and coccoid morphotypes have been implicated in lithification of Type 3 mats. Phylogenetic analysis identified only 1% of the sequences from the stomatrolite libraries with > 95% identity to known cyanobacterial sequences in GenBank. These sequences are all related to the pleurocapsalean cyanobacteria *Xenococcus* sp., also observed in Shark Bay stromatolites (Burns *et al.*, 2005) and *Chroococcidiopsis* sp., which occur in Antarctic endolithic communities (Fewer *et al.*, 2002).

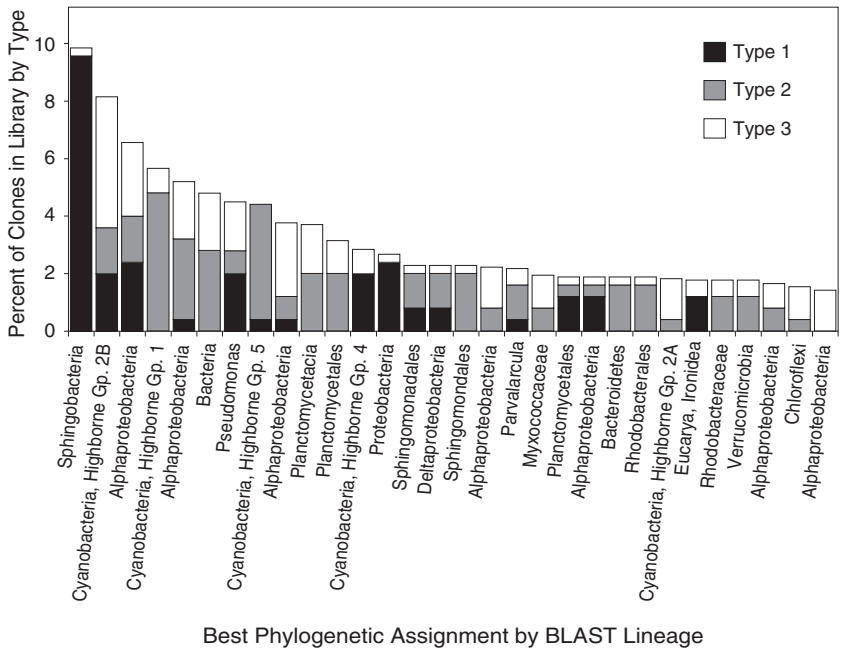

Fig. 5. Rank abundance of most abundant (> 5 clones total) OTUs from the stromatolite communities. The per cent of the library from each mat type represented in each OTU is indicated by shading consistent with the key provided in the figure. The most exact taxonomic affiliation possible as determined by BLAST to the NCBI database is provided. Cyanobacterial associations noted correspond to Fig. S1.

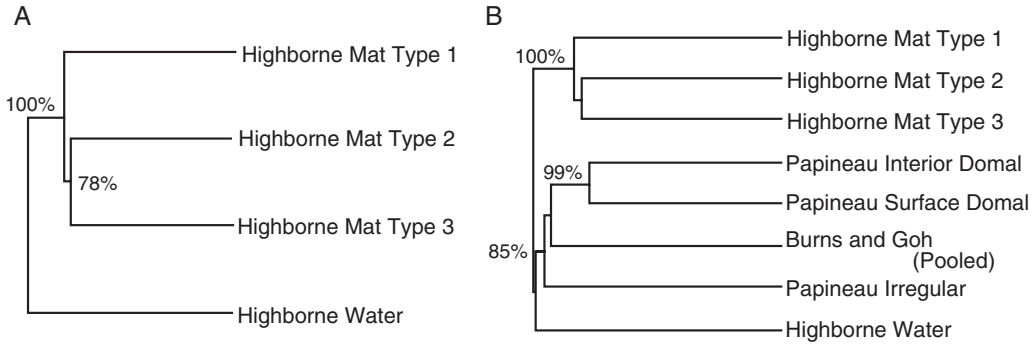

Fig. 6. Jackknifed UPGMA trees from UniFrac that represent similarities in mat community composition for Highborne Cay stromatolites (A), and for Highborne Cay stromatolites in relation to stromatolites in Hamelin Pool, Australia (B) as described in Burns and colleagues (2004), Goh and colleagues (2006) and Papineau and colleagues (2005). Numbers represent the per cent of 1000 replicate trees in which the indicated node was present. Both trees were constructed with 70 randomly subsampled sequences from each library, which was restrained by the library from the Highborne Cay water sample (similar topologies and values were achieved with the water library excluded and the libraries subsampled at 250 sequences).

The majority of the remaining cyanobacterial sequences from stromatolite samples comprised two groups (Fig. S1). The first group, which we refer to as Highborne Group 1, included representatives of the pleurocapsales with $\leq$ 94% identity to existing sequences. A single OTU from this group was abundant in the stromatolite libraries and occurred in all three mat types (Fig. 5). The second group, Highborne Group 2, had identities of no more than 92% to known sequences. A single OTU from this group was found in all three mat types and represented the second most frequently observed OTU in the stromatolite communities (Fig. 5). Although distantly related, the sequences that share the most similarity to Highborne Group 2 are from the *Oscillatoria*, which include many of the filamentous *Cyanobacteria* previously identified by microscopic observations in the stromatolites (i.e. genera *Schizothrix*, *Microcoleus*) (Fig. S1). A third novel group of *Cyanobacteria*, Highborne Group 5, was conspicuous in the stromatolite libraries, but was almost exclusively found in mat Type 2 (Fig. 5, Fig. S1).

Sulfate-reducing bacteria, as well as cyanobacteria, have been implicated in carbonate precipitation and lithification (Baumgartner *et al.*, 2006). Sequences specifically related to known sulfate-reducing *Deltaproteo-*

Table 3. Abundance of major phyla recovered in clone libraries from each stromatolite type and water samples.

	Percentage of sequences in library				
	Type 1	Type 2	Type 3	Water	% of all libraries
Bacteria	95.2	99.2	95.7	100.0	97.0
Proteobacteria	41.3	57.4	52.8	66.2	52.0
Alphaproteobacteria	32.1[a]	49.0	41.8	56.3	42.3
Deltaproteobacteria	3.2	6.4	6.0		4.9
Gammaproteobacteria	6.0	2.0	5.1	9.9	4.9
Planctomycetes	14.3	11.2	13.4	1.4[b]	12.1
Cyanobacteria	10.3	14.3	9.9	14.1	11.6
Bacteroidetes	17.5	7.6[c]	6.0[d]	16.9	10.4
Chloroflexi	2.4	2.4	5.7	1.4	3.6
Spirochaetes	2.4	0.8	2.8		1.9
Verrucomicrobia	2.4	2.4	0.9		1.6
Actinobacteria	2.4		0.3		0.8
Firmicutes	0.4	1.2	0.3		0.5
Chlorobi			0.9		0.3
Deferribacteres	0.8				0.2
Other *Bacteria*	2.0	1.2	2.8		1.9
Archaea total		0.8	1.4		0.8
Eukarya total	4.4		2.8		2.3

Footnotes are used to denote differences between libraries found to be significant by pairwise comparison with Fisher's exact test:
a. *Alphaproteobacteria* are less abundant in Type 1 mats than in either Type 2 mats ($P = 0.0002$) or water samples ($P = 0.0003$).
b. *Planctomycetes* are less abundant in water samples than in either Type 1 ($P = 0.0012$), 2 ($P = 0.0086$), or Type 3 ($P = 0.0017$) mats.
c. *Bacteroidetes* are less abundant in Type 2 than in Type 1 mats ($P = 0.0011$).
d. *Bacteroidetes* are less abundant in Type 3 mats than in either Type 1 mats ($P = 0.0001$) or water samples ($P = 0.0056$).

bacteria were not abundant in any of the clone libraries and there were no sequences representative of known sulfate-reducing bacteria or archaea (Table 3). Only three groups of SSU rRNA sequences related to known sulfate-reducing *Deltaproteobacteria* were observed in the stromatolites: *Desulfobacteria* spp. (one sequence in the Type 1 library and four sequences in the Type 3 library), *Desulfomonile* spp. (one sequence in the Type 1 library), and *Desulfovibrio* spp. (three sequences each in the Type 2 and Type 3 libraries). None of these sequences is closely related to those from cultured organisms from this site (GenBank Accession No. DQ822785–DQ822789). As with the cyanobacterial sequences, the putative sulfate-reducing deltaproteobacterial sequences were not closely related to sequences in GenBank ($\leq$ 93% identity).

Discussion

Stromatolite-forming microbial mat communities at Highborne Cay cycle through three morphologically conspicuous stages of development, generally with the sequence 1–2–3–1 or 1–2–1 (Reid *et al*., 2000; Visscher *et al*., 2000). Our results show that the taxonomic richness of the stromatolite mat communities increases and community composition changes dramatically as the community develops through the three different mat types. Type 1 communities are the least diverse (Figs 4 and 5, Tables 2 and 3) and have significantly lower sulfate reduction rates (Fig. 4, Table 1), which is consistent with the premise that sulfate reduction is a driver of lithification in the Type 2 and 3 mats. Additionally, the community compositions and biogeochemistry of the lithifying Type 2 and Type 3 mats are fairly similar and differ significantly from these characteristics in the Type 1 mats (Figs 5 and 6, Table 3).

Cyanobacteria are expected to contribute to primary productivity and are hypothesized to promote lithification in the stromatolite system. Indeed, cyanobacterial sequences are abundant in the Highborne Cay stromatolite libraries (10–14%). Previous microscopy-based studies have identified *Schizothrix* sp. and *Solentia* sp. as key cyanobacterial species that contribute to the sediment structure of the Highborne Cay stromatolites (e.g. Macintyre *et al*., 2000; Reid *et al*., 2000). However, sequences from *Schizothrix* sp. were not detected in stromatolite libraries, and SSU rRNA sequences are not yet available for cultured *Solentia*. Thus, one of the novel groups of cyanobacteria detected in the stromatolites may represent or morphologically resemble either of these previously identified cyanobacteria. Regardless, the cyanobacterial sequences average only ~93% identity to known cyanobacteria. This shows that the stromatolites are home to novel genera of cyanobacteria that merit further characterization.

Sulfate-reducing bacteria also are hypothesized to play a key role in the precipitation of calcium carbonate (e.g. Visscher *et al*., 1998; 2000; Visscher and Stolz, 2005; Baumgartner *et al*., 2006), and the involvement of sulfate-reducing bacteria in these types of reactions has been documented (Lyons *et al*., 1984; Walter *et al*., 1993; van Lith *et al*., 2003). The majority of the classically studied sulfate-reducing bacteria are phylogenetically associated with the *Deltaproteobacteria*. The current study did not reveal major differences in deltaproteobacterial diversity between the three mat types, and relatively few deltaproteobacterial sequences appear in any of the libraries. Additionally, there are no sequences in the libraries indicating close relatives of the other known sulfate-reducing bacteria or archaea. It should be noted that the oxygen concentration typically present at the surface of Type 2 mats (where the highest sulfate-reducing bacterial abundance and activity are observed) is between 80% and 150% of air saturation. The abundance, distribution and metabolic rates of sulfate-reducing bacteria in surface mats are still poorly understood (Cypionka, 2000; Baumgartner *et al*., 2006). However, both the high rates of sulfate reduction in the oxic surfaces of the stromatolites (Visscher *et al*., 2000) and the concentration of ^{13}C in microcrystalline carbonate precipitates in Type 2 mats (Andres *et al*., 2006) strongly suggest the involvement of sulfate-reducing bacteria in the stromatolite formation. The combined data suggest two alternatives. First, a few specialized species of sulfate-reducing bacteria capable of high rates of sulfate reduction are active at the stromatolite surface and catalyse lithification of Type 2 mats through formation of micritic (microcrystalline) crusts. As has been proposed in other systems, these species would be adapted to relatively high oxygen concentrations, or form consortia (e.g. with sulfur- or sulfide-oxidizing bacteria) that limit oxygen exposure (Baumgartner *et al*., 2006; Stephen *et al*., 2008). It should be noted that sulfur oxidation is common throughout the phylogenetic tree, from the lone known archaeal genera (*Sulfolobus*), to a wide range of *Bacteria*, including *Aquificales*, *Chlorobi*, and a wide spread of *Proteobacteria* (Friedrich *et al*., 2001). A second possibility, given that many of the sequences in the libraries were not closely related to any cultured organisms, is that other phylogenetic groups have the ability to reduce sulfate.

Species richness and lithification both increase with each stage in stromatolite community development. Whether there is a link between these two characteristics remains unclear, although there are reasons to postulate such a relationship. For example, the fused grains observed in the Type 3 mats are caused by interrelationships between a boring cyanobacterium that produce EPS and heterotrophs that feed on the EPS (Reid *et al*., 2000; Visscher *et al*., 2002). Thus, increases in richness

of functional groups that mediate EPS production or consumption in the mat can influence lithification (Dupraz and Visscher, 2005). Alternatively, greater taxonomic richness could correspond to a greater diversity of metabolic types in the mat, potentially altering mat biogeochemistry and/or increasing productivity (Caspersen and Pacala, 2001), which in turn may facilitate lithification.

Microbial mats, including stromatolites, are the oldest ecosystems known. Commonalities among modern marine analogues of ancient stromatolites may provide keys to understanding the formation and biogeochemistry of ancient stromatolites. Studied modern analogues are found in the Exuma Cays of the Bahamas (including Highborne) and in Shark Bay, Australia. Stromatolites in Shark Bay share some characteristics with Highborne Cay stromatolites (Burns *et al*., 2004; 2005; Papineau *et al*., 2005; Goh *et al*., 2006), and the rRNA gene libraries from the Shark Bay and Highborne Cay stromatolites have some similarities at the phylum level. However, UniFrac analysis showed that the communities are distinct in their composition (Fig. 6B). Differences in community composition could result from geographic isolation or from physical, chemical or other environmental differences. For instance, Highborne stromatolites form in a high-energy, wave-dominated, subtidal system, while Shark Bay stromatolites form within a protected tidal zone. Beyond the differences driven by physical environment, the kinds of organisms that are similar in these modern stromatolite communities possibly were also active in and responsible for the ancient stromatolites.

This study provides a molecular perspective on the composition of the well-studied stromatolites of Highborne Cay. These results reinforce the previously proposed model for formation of the stromatolites and document many novel microorganisms. The results also highlight the utility of further characterization of both the cyanobacteria and sulfate-reducing bacteria in these systems.

Experimental procedures

Sample collection

Stromatolite and water samples were collected at Highborne Cay, Exumas, Bahamas (24°43′N, 76°49′W) on 23 and 24 July 2004. Five to six samples were taken from subtidal stromatolites with surface communities representing each of the three mat types. Surface mats were immediately dissected and subsampled in the laboratory of the R/V Walton Smith. For molecular analysis, the surface layer (0.5–3 mm) was aseptically sectioned under a dissecting microscope. These sections were mechanically homogenized, frozen in liquid nitrogen, and maintained at –80°C until the sample was extracted. A piece of each stromatolite sample was also preserved in a 4% formaldehyde solution for imaging.

Water samples from the stromatolite site were collected in new 0.5 l Nalgene bottles. The samples were then filtered onto a 0.22 μm polyethersulfone filter (Stericup, Millpore), and the filter was removed and frozen in liquid nitrogen. Samples were kept on liquid nitrogen for transport back to the lab, where they were stored at –80°C until analysed.

Geochemical and microbial rate measurements

Type 1, 2 and 3 mats were sampled twice per year during 2003–2007. The intensity of photosynthetically active radiation (PAR) at the mat surface *in situ* was measured with a Licor LI-250 meter equipped with an underwater quantum sensor (LI-192). The salinity was determined using a hand-held refractometer (Fisher Scientific) and the water temperature and pH using a hand-held meter (Hannah HI 9024, Hannah Instruments, RI). Microelectrode profiles of oxygen and sulfide were taken either *in situ* using a Unisense (Denmark) tethered benthic lander device or in fresh samples that were incubated at ambient light and water temperature with microelectrodes attached to a motor-driven micromanipulator (National Aperture, NH) (Visscher *et al*., 1998; 2002). Oxygen concentrations were measured using calibrated polarographic sensors equipped with a guard cathode (tip diameter 60 μm; Unisense, Denmark) and a picoammeter (Unisense PA2000). Sulfide and pH microprofiles were measured with ion-selective microelectrodes (Diamond General, MI, and Microscale Measurements, the Netherlands respectively) and a high-impedance mV meter (Microscale Measurements, the Netherlands). Profiles in the top 20 mm were measured in 250 μm increments. Profile measurements were replicated four times. Depth profiles of photosynthesis and aerobic respiration rates were calculated from oxygen microelectrode measurements during the peak of photosynthesis (i.e. between noon and 2:00 PM) using the light-dark shift method (Visscher *et al*., 1998; 2002).

The rate of sulfate reduction was measured in vertically cut samples using 2×5 cm strips of $^{35}SO_4^{2-}$-labelled silver foil (Visscher *et al*., 2000). The $^{35}SO_4^{2-}$ is reduced to $^{35}S^{2-}$, which precipitates to $Ag^{35}S$ on the foil surface and can be visualized as pixel pattern by radiography. Pixel patterns were calibrated using traditional $^{35}SO_4^{2-}$ incubations in homogenates of separated mat layers, using the single-step chromium reduction technique (Visscher *et al*., 2000; 2002).

Molecular analysis

Mat samples were obtained from surface communities on multiple stromatolite heads (six samples were obtained per mat type for Type 1 and 2 communities while five were obtained for Type 3 communities). All samples were extracted with the FastDNA Spin Kit for Soil (QBiogene) according to manufacturer's instructions, except that 1.5 min of beadbeating was substituted for the 0.5 min of FastSpin. Each mat sample was mechanically homogenized with a pipette tip and then extracted in triplicate, using 0.19–0.25 g per DNA extraction. The filter from the water sample was cut into eighths (5 mm^2 each). One eighth of the filter was used for each DNA extraction, and 80 μl of chloroform was added to the Lysing Matrix tube with the sodium phosphate buffer to dissolve the filter before extraction with FastDNA Spin Kit for Soil. The extracted SSU rDNA from each sample was amplified via PCR with a universal primer pair that targets *Bacteria*,

Archaea and *Eukarya* (515F and 1391R; Lane, 1991). Polymerase chain reaction was conducted according to previously published methods (Singleton *et al*., 2001). DNA was extracted from each stromatolite sample individually, and three PCR reactions were performed for each DNA extract (Type 1 and 2, 18 total PCR reactions per mat type, Type 3, 15 PCR reactions). The resulting PCR products were pooled by mat type. The pooled PCR product was cloned, screened by restriction fragment length polymorphism (RFLP) and sequenced as previously described (Spear *et al*., 2005). The clone libraries generally contained > 30 RFLP different patterns and all clones from each 96-well plate were sequenced.

Sequence analysis

Raw sequences were assembled into contiguous sequences in Xplorseq (Frank, 2008), then compared with the GenBank database by the basic local alignment search tool (BLAST) (Altschul *et al*., 1990). Contiguous sequences with BLAST bit scores of over 500 and lengths > 300 bp were aligned with the NAST aligner to a database of > 75 000 near full-length (> 1250 nucleotides) sequences (DeSantis *et al*., 2003; 2006). Aligned sequences were imported into the ARB software package (Ludwig *et al*., 2004). Potential chimeric sequences were identified by long branch length in ARB and checked by examining each end of the sequence with the BLASTN function on the NCBI website (Altschul *et al*., 1990). If the two ends of the sequence generated BLAST hits from different genera, it was classified as a chimera and excluded from further analysis. Remaining sequences were checked with Bellerophon (Huber *et al*., 2004) and no chimeras were found.

Differences in diversity between sequences from each library were analysed with UniFrac (Luzapone and Knight, 2005) and ∫-LibShuff (Singleton *et al*., 2001; Schloss *et al*., 2004). Expected diversity from each library was calculated with EstimateS (Colwell, 2005). Matrices for EstimateS were filtered with lanemaskPH to remove distance caused by hypervariable regions (provided with ARB database; Hugenholtz, 2002). For the EstimateS calculations, we used 11 OTU definitions, from 90% to 100% sequence identity, and we report the results from the 97% identity OTU (approximately species level; Stackebrandt and Goebel, 1994). Chao1 was calculated using the classic formula in EstimateS (Chao, 1984). Boostrap analyses were conducted in RAxML (Stamatakis, 2006). DOTUR (Schloss and Handelsman, 2005) and sortX (as part of the Xplorseq package, Frank, 2008) analyses were conducted using furthest neighbour at 97% OTU. These sequence data have been submitted to the GenBank database under Accession No. FJ911911–FJ912833 (the subset of sequences utilized in DOTUR analysis are under Accession No. FJ911975–FJ912833). The second character of each sequence name reflects the source sample: W for water, and numbers 1, 2 or 3 for microbial mat Types 1, 2 and 3 respectively.

Acknowledgements

This work was supported by the National Science Foundation (Biocomplexity Program EAR-0221796 and Biogeosciences Program 0311929). L. Baumgartner would like to thank J. Kirk Harris, Daniel Frank and Charles Robertson for their assistance with various aspects of phylogenetic analysis, and Kristen Przekop for culturing sulfate-reducing bacteria from the site. Research Initiative on Bahamian Stromatolites (RIBS) Contribution #57 and UConn's Center for Integrative Geoscienes #15.

References

Altschul, S.F., Gish, W., Miller, W., Myers, E.W., and Lipman, D.J. (1990) Basic local alignment search tool. *J Mol Biol* **215:** 403–410.

Andres, M.S., Sumner, D.Y., Reid, R.P., and Swart, P.K. (2006) Isotopic fingerprints of microbial respiration in aragonite from Bahamian stromatolites. *Geology* **34:** 973–976.

Baumgartner, L.K., Reid, R.P., Dupraz, C., Decho, A.W., Buckley, D.H., Spear, J.R. *et al.* (2006) Sulfate reducing bacteria in microbial mats: changing paradigms, new discoveries. *Sediment Geol* **185:** 131–145.

Braissant, O., Decho, A.W., Dupraz, C., Glunk, C., Przekop, K.M., and Visscher, P.T. (2007) Exopolymeric substances of sulfate-reducing bacteria: interactions with calcium at alkaline pH and implications for formation of carbonate minerals. *Geobiology* **5:** 401–411.

Burns, B.P.F., Goh, M., Allen, M., and Neilan, B.A. (2004) Microbial diversity of extant stromatolites in the hypersaline marine environment of Shark Bay, Australia. *Environ Microbiol* **6:** 1096–1101.

Burns, B.P., Seifert, A., Goh, F., Pomati, F., Yasar, S.A., and Neilan, B.A. (2005) Genetic potential for secondary metabolite production in stromatolite communities. *FEMS Microbiol Lett* **243:** 293–301.

Caspersen, J.P., and Pacala, S.W. (2001) Successional diversity and forest ecosystem function. *Ecol Res* **16:** 895–903.

Chao, A. (1984) Non-parametric estimation of the number of classes in a population. *Scand J Stat* **11:** 265–270.

Colwell, R.K. (2005) *EstimateS: statistical estimation of species richness and shared species from samples*, Version 7.5 [WWW document]. URL http://purl.oclc.org/estimates.

Cypionka, H. (2000) Oxygen respiration by *Desulfovibrio* species. *Annu Rev Microbiol* **54:** 827–848.

Decho, A.W., Visscher, P.T., and Reid, R.P. (2005) Production and cycling of natural microbial exopolymers (EPS) within a marine stromatolite. *Palaeogeogr Palaeoclimatol Palaeoecol* **219:** 71–86.

DeSantis, T.Z., Dubosarskiy, I., Murray, S.R., and Andersen, G.L. (2003) Comprehensive aligned sequence construction for automated design of effective probes (CASCADE-P) using 16S rDNA. *Bioinformatics* **19:** 1461–1468.

DeSantis, T.Z., Hugenholtz, P., Keller, K., Brodie, E.L., Larsen, N., Piceno, Y.M., *et al.* (2006) NAST: a multiple sequence alignment server for comparative analysis of 16S rRNA genes. *Nucleic Acids Res* **34:** W394–W399.

Dupraz, C., and Visscher, P.T. (2005) Microbial lithification in marine stromatolites and hypersaline mats. *Trends Microbiol* **13:** 429–438.

Fewer, D., Friedl, T., and Büdel, B. (2002) *Chroococcidiopsis* and heterocyst-differentiating cyanobacteria are each other's closest living relatives. *Mol Phylogenet Evol* **23:** 82–90.

Frank, D.N. (2008) XplorSeq: a software environment for integrated management and phylogenetic analysis of metagenomic sequence data. *BMC Bioinformatics* **9:** 1–16.

Friedrich, C.G., Rother, D., Bardischewsky, F., Quentmeier, A., and Fischer, J. (2001) Oxidation of reduced inorganic sulfur compounds by bacteria: emergence of a common mechanism? *Appl Environ Microbiol* **67:** 2873–2882.

Goh, F., Leuko, S., Allen, M.A., Bowman, J.P., Kamekura, M., Neilan, B.A., and Burns, B.P. (2006) *Halococcus hamelinensis* sp. nov., a novel halophilic archaeon isolated from stromatolites in Shark Bay, Australia. *J Syst Evol Microbiol* **56:** 1323–1329.

Huber, T., Faulkner, G., and Hugenholtz, P. (2004) Bellerophon; a program to detect chimeric sequences in multiple sequence alignments. *Bioinformatics* **20:** 2317–2319.

Hugenholtz, P. (2002) Exploring prokaryotic diversity in the genomic era. *Genome Biol* **3:** reviews0003.1–0003.8.

Lane, D.J. (1991) 16S/23S rRNA sequencing. In *Nucleic Acid Techniques in Bacterial Systematics.* Stackebrandt, E., and Goodfellow, M. (eds). New York, USA: Wiley, pp. 115–175.

van Lith, Y., Warthmann, R., Vasconcelos, C., and McKenzie, J.A. (2003) Sulphate-reducing bacteria induce low-temperature Ca-dolomite and high Mg-calcite formation. *Geobiology* **1:** 71–79.

Ludwig, W., Strunk, O., Westram, R., Richter, L., Meier, H., Yadhukumar, A., *et al.* (2004) ARB: a software environment for sequence data. *Nucleic Acids Res* **32:** 1363–1371.

Luzapone, C., and Knight, R. (2005) UniFrac: a new phylogenetic method for comparing communities. *Appl Environ Microbiol* **71:** 8228–8235.

Lyons, W.B., Long, D.T., Hines, M.E., Gaudette, H.E., and Armstrong, P.B. (1984) Calcification of cyanobacterial mats in Solar Lake, Sinai. *Geology* **12:** 623–626.

Macintyre, I.G., Prufert-Bebout, L., and Reid, R.P. (2000) The role of endolithic cyanobacteria in the formation of lithified laminae in Bahamian stromatolites. *Sedimentology* **47:** 915–921.

Papineau, D., Walker, J.J., Mojzsis, S.J., and Pace, N.R. (2005) Composition and structure of microbial communities from stromatolites of Hamelin Pool in Shark Bay, Western Australia. *Appl Environ Microbiol* **71:** 4822–4832.

Reid, R.P., Visscher, P.T., Decho, A.W., Stolz, J.F., Bebout, B.M., Dupraz, C., *et al.* (2000) The role of microbes in accretion, lamination and early lithification of modern marine stromatolites. *Nature* **406:** 989–992.

Schloss, P.D., and Handelsman, J. (2005) Introducing DOTUR, a computer program for defining operational taxonomic units and estimating species richness. *Appl Environ Microbiol* **71:** 1501–1506.

Schloss, P.D., Larget, B.R., and Handelsman, J. (2004) Integration of microbial ecology and statistics: a test to compare gene libraries. *Appl Environ Microbiol* **70:** 5485–5492.

Singleton, D.R., Furlong, M., Rathbun, S.L., and Whitman, W.B. (2001) Quantitative comparisons of 16S rRNA gene sequence libraries from environmental samples. *Appl Environ Microbiol* **67:** 4374–4376.

Spear, J.R., Walker, J.J., McCollom, T.M., and Pace, N.R. (2005) Hydrogen and bioenergetics in the Yellowstone geothermal ecosystem. *Proc Natl Acad Sci USA* **102:** 2555–2560.

Stackebrandt, E., and Goebel, B.M. (1994) Taxonomic note: a place for DNA–DNA hybridization and 16S rRNA sequence analysis in the present species definition in bacteriology. *Int J Syst Bacteriol* **44:** 846–849.

Stamatakis, A. (2006) RAxML-VI-HPC: maximum likelihood-based phylogenetic analyses with thousands of taxa and mixed models. *Bioinformatics* **22:** 2688–2690.

Stephens, E., Braissant, O., and Visscher, P.T. (2008) Spirochetes and salt marsh microbial mat geochemistry: implicatiuons for the fossil record. *Notebooks Geol* **CG2008_AO9:** 1–11.

Visscher, P.T., and Stolz, J.F. (2005) Microbial mats as bioreactors: populations, processes, and products. *Palaeogeogr Palaeoclimatol Palaeoecol* **219:** 87–100.

Visscher, P.T., Reid, R.P., Bebout, B.M., Hoeft, S.E., Macintyre, I.G., and Thompson, J.A., Jr (1998) Formation of lithified micritic laminae in modern marine stromatolites (Bahamas): the role of sulfur cycling. *Am Mineralogist* **83:** 1482–1494.

Visscher, P.T., Reid, R.P., and Bebout, B.M. (2000) Microscale observations of sulfate reduction: correlation of microbial activity with lithified micritic laminae in modern marine stromatolites. *Geology* **28:** 919–922.

Visscher, P.T., Hoeft, S.M., Surgeon, T.L., Rogers, D.R., Bebout, B.M., Thompson, J.S., and Reid, R.P. (2002) Microelectrode measurements in stromatolites: unraveling the Earth's past? In *Environmental Electrochemistry: Analyses of Trace Element Biogeochemistry.* ACS Symposium Series. Taillefert, M., and Rozan, T. (eds). Washington, DC, USA: Oxford University Press, pp. 265–282.

Walter, L.M., Bischof, S.A., Patterson, W.P., and Lyons, T.W. (1993) Dissolution and recrystallization in modern shelf carbonates: evidence from pore water and solid phase chemistry. *Phil Trans R Soc A* **344:** 27–36.

Zhang, J.-Z. (2000) Oxidation of hydrogen sulfide by various oxidants in natural waters. *Trends Geochem* **1:** 53–68.

Supporting information

Additional Supporting Information may be found in the online version of this article:

Fig. S1. The Highborne Cay cyanobacterial sequences and other representative sequences in a neighbour-joining tree from ARB. Numbers are bootstrap values from 1000 trees in RAxML, and all branches not supported by bootstrap (< 70%) have been removed. Taxonomic groups are indicated on the right. The sequence source for Highborne Cay sequences is indicated in the name: H1, Type 1; H2, Type 2; H3, Type 3; HW, water.

Please note: Wiley-Blackwell are not responsible for the content or functionality of any supporting materials supplied by the authors. Any queries (other than missing material) should be directed to the corresponding author for the article.